

SECONDARY ELECTRON YIELD OF SURFACES: WHAT WE KNOW AND WHAT WE STILL NEED TO KNOW

M. Taborelli, CERN European Organization of Nuclear Research, Geneva, Switzerland

Abstract

The electron cloud phenomenon in particle accelerators is related to the secondary electron yield of the surfaces in line of sight of the beam. At present, advanced models to predict electron cloud through simulation codes are available and they rely either on experimental data or on parametrizations of the various quantities and dependencies describing the behaviour of electrons impinging on and emitted from the surface. In the present contribution, we review what is well established about these dependencies and which measurements should still be performed.

INTRODUCTION

It is well accepted that the Total or the Secondary Electron Yield (TEY, SEY) of the exposed surfaces is one of the main quantities governing electron cloud and multipacting. Powerful simulation algorithms have been developed with the aim of predicting the maximum operating power of RF devices [1] or the maximum stable particle beam intensity [2]. The algorithms must rely on the physics of the generation and emission of secondary electrons from solids. Ideally for a simulation, the quantity $I(E_s, \theta_{emis}, E_p, \theta_{inc})$ is necessary for the relevant range of energies and angles, where I is the emitted electron intensity for a fixed impinging intensity, E_p is the kinetic energy of the impinging electrons with respect to the vacuum level of the surface, θ_{inc} is the angle of incidence, E_s the energy of emission and θ_{emis} the angle of emission.

Even if the fundamental principles of electron scattering are known, there are no simple exact analytical expressions for the various energy and angle dependencies. Only recently calculations of the yields based for instance on dielectric theory [3, 4, 5], can predict the absolute TEY(E_p) of ideally clean and pure surfaces including a basic model of surface roughness [3]. These are different from the air exposed oxidised and contaminated surface of real devices. The values and shapes of the curve of TEY for a material can change markedly depending on its surface state. For instance for OFE copper the TEY curve can change over a wide range: a typical as-received (air exposed and chemically cleaned for UHV applications) surface of technical copper will have a δ_{max} around 2.0 [6], a freshly electropolished surface has a value of 1.6 [7], but a rough surface can [8] exhibit a δ_{max} as low as 1.0. These values differ significantly from the value of 1.4 [6] for a sputter cleaned surface in vacuum. It is interesting to remark that the range of values mentioned just above cover the range of δ_{max} including those leading to severe e-cloud down to those which suppress e-cloud in accelerators. Therefore, the electron cloud simulations use experimental data, when available, or parametrizations based on the ex-

perimental data, which are in some cases supported by phenomenological models. Typically, parametrizations are used for the primary electron energy dependence of the TEY, for its dependence on impinging electron angle and for the energy and angle distribution of the emitted electrons. Another variable, which influences the TEY, is the history of the surface in terms of received electron or photon irradiation dose and this cannot be directly included in a parametrization.

The present contribution is a tentative to illustrate what is available and how well it describes the real situation. Only metal surfaces will be discussed, since they are the most relevant in the case of particle accelerators.

TEY, PARAMETRIZATION AND MEASUREMENT

1. TEY parametrization:

The TEY(E_p, θ_{inc}) is the ratio between the total number of electrons emitted by the surface and the number of electrons impinging at an angle θ_{inc} and energy E_p . For the emitted electrons the simplest distinction can be made between elastically scattered electrons, $El(E_p)$, emitted at the same energy as E_p , and those emitted at lower energy, which were excited or scattered inelastically, $SEY(E_p)$ (some authors introduce in addition the backscattered electrons, which are in the present case included in the SEY for simplicity). This leads to (we skip in the following of this section θ_{inc} taken as fixed, for instance as zero for normal incidence):

$$TEY(E_p) = SEY(E_p) + El(E_p) \quad (1)$$

In several phenomenological models the values of the maximum of the TEY(E_p), δ_{max} and the energy at which the maximum occurs, E_{max} , are used to fully characterize the curve and enable a scaling of the SEY(E_p) curve (examples in [9, 10]) with respect to normalised variables:

$$\frac{SEY(E_p)}{\delta_{max}} = g\left(\frac{E_p}{E_{max}}\right) \quad (2)$$

However, $g(x)$ depends on the surface condition (chemistry, roughness) and a technical surface of an accelerator component is composed of several layers (the underlying metal, an oxide layer, some surface contamination...). In practice the parametrization of the experimental SEY curve with more variables is used, as for instance [11]:

$$\frac{SEY(E_p)}{\delta_{max}} = \frac{s \frac{E_p}{E_{max}}}{s-1 + \left(\frac{E_p}{E_{max}}\right)^s} \quad (3)$$

Where s is a fit parameter, often chosen in the range 1.35-1.45.

The relevant range of E_p is limited to about 1keV, corresponding to the maximum energy of the electrons impinging on the beampipe, except for machines which very short and highly charged pulses as the J-Parc accelerator, where the relevant range rises up to some keV [12]. On the other side, at low primary energy, below some tens of eV, the possible excitation channels for secondary electrons decrease and the elastic electrons contribution $El(E_p)$ plays an important role. They must therefore be added to the $SEY(E_p)$ to get the curve $TEY(E_p)$.

Two approaches are common [13, 14] for the parametrization of $El(E_p)$. The first approach starts from the reflectivity of a free electron wave function at a one-dimensional step-like barrier (the surface). In order to match experimental data, the barrier height E_0 must assume values, which are very high (as 150eV) compared with typical work function values. A further coefficient R_0 is added to tune the reflectivity at zero kinetic energy. So, the resulting yield of elastic electrons is:

$$El(E_p) = R_0 \left(\frac{\sqrt{E_p} - \sqrt{E_p + E_0}}{\sqrt{E_p} + \sqrt{E_p + E_0}} \right)^2 \quad (4)$$

Where R_0 and E_0 are fit parameters. In a second approach the experimental data are fitted with a multi-parameter development in powers of $\ln(E_p)$:

$$\begin{aligned} \ln f &= \\ &= 1.59 + 3.75 \ln E_p - 1.37 (\ln E_p)^2 + 0.12 (\ln E_p)^3 \end{aligned} \quad (5)$$

Where the numerical coefficients are those reported in the reference [14] for “universal function” and f is the fraction of elastic electrons:

$$E_l(E_p) = f \cdot TEY(E_p) \quad (6)$$

or in an equivalent way:

$$TEY(E_p) = \frac{SEY(E_p)}{1-f} \quad (7)$$

In fact the coefficients in (5) are material dependent and different values were used for instance for copper [15].

The importance of acquiring experimental data on a specific individual sample is clear when considering the difficulties to extrapolate from first principle calculations or parametrization. At present there is no model, which can deliver the correct TEY curve starting from a given surface composition, roughness and received dose.

2. TEY measurements:

In experimental measurements the $TEY(E_p)$ and $SEY(E_p)$ are often used with equivalent meaning, since

above a primary energy of some 100 eV the main contribution to the yield is given by secondary electrons and only recently measurements are common below 100eV. In particular, since the maximum, δ_{max} , is generally above 200 eV, we can consider that the maximum of TEY and SEY is the same within a negligible error. In principle, the aim of the experiments is to measure the primary energy dependence of all emitted electrons, the TEY, since all of them contribute to the multipacting effects.

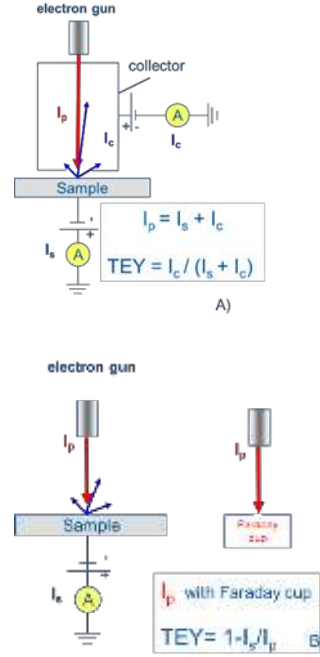


Figure 1: Sketch of the most common measuring modes for the electron yield: A) With a collector, to measure simultaneously the absorbed and emitted current. B) Without collector and with the total impinging current measured either by a Faraday cup or by reversing the bias. The symbols represent total primary current I_p , sample current I_s , collector current I_c and electron yield TEY.

Most of the measurements for simplicity are performed at normal incidence ($\theta_{inc} = 0$). TEY curves are acquired routinely in several laboratories for primary energies above 100eV. Recently the measurements of the very low primary energy part of the TEY curve in several labs have achieved reliability down to few eV (measuring in this range is made difficult by the sensitivity of slow electrons to parasitic electric and magnetic fields). The instruments measuring the TEY are based on an electron gun at variable energy and a sample facing the gun. They can be divided in two main categories: a) those measuring simultaneously the current absorbed by the sample and the current emitted by the surface in a collector [6] and b) those measuring in separate runs the current absorbed by the sample and the total current from the electron gun. In the first method a negative bias of few volts constantly applied on the sample helps to avoid recollection of the slow secondary electrons on the sample. The total emitted current is measured simultaneously in a collector, which is

mounted between gun and sample and is coaxial to the gun. In the second method the absorbed current is measured in the same way as in the first case, but the total current is obtained separately, either through a Faraday cup or by applying a sufficiently high positive bias to attract all the electrons on the sample. The two methods are sketched in figure 1. The method of measurement without collector sacrifices the advantage of measuring simultaneously the necessary currents, but gains the advantage of enabling measurements at very low primary energy by placing the electron source close to the sample surface [16], which is important for measurements at low kinetic energy. A more complex scheme based on time-of-flight is presently under development for measurements in a magnetic field [17]. In the case of air exposed samples, which is the initial typical condition for components installed in an accelerator, it is important to keep a low dose of irradiation on the sample. It is well known that for air exposed samples the TEY value starts to decrease for doses above 10^{-6} C/mm² at impinging energies above 50eV [18]. In order to limit the delivered dose during measurements the beam is pulsed or deviated away from the surface before and after each point of data acquisition. The methods of measurement described above provide a precise, but not accurate value of the absolute yield, as explained in the following. The typical relative error, generated by the relative error on the measured currents, on a single curve is of few % of TEY (typically better than 0.05 for a yield in the usual range, namely below 2). This means that the reproducibility (precision) on a sample spot is very high and this enables for instance to identify weak differences in SEY of about 0.1 in neighbouring regions of the same sample [19]. However, the absolute value of the TEY cannot be measured with the same accuracy and depends slightly on the geometry of the measuring device, which influences the efficiency of the collection of electrons at the various energies. The accuracy in this case is rather around 10% , depending on the considered E_p . An example of the difference between two measuring devices is shown in figure 2.

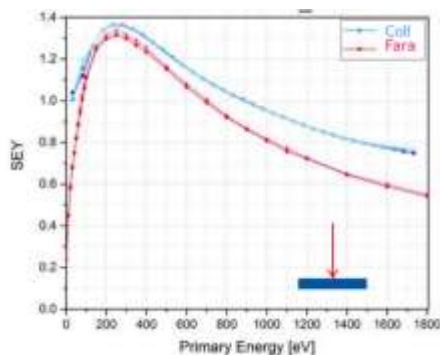


Figure 2: Secondary electron yield curves for a thin film of carbon as a function of primary energy for the same sample measured with a collector system and a Faraday cup system.

For this reason comparison between different laboratories should be taken with care. Even defining a suitable reference sample to compare devices is not a simple task,

possible candidates being amorphous carbon coatings, which are rather insensitive to air exposure or surfaces prepared in situ in vacuum with a very well defined procedure.

The vacuum system of several modern accelerators, as for example the beamscreen of the arcs of LHC (5-20 K), operates at cryogenic temperature, because of the use of superconducting magnets. The SEY of a copper surface at low temperatures has been shown to have the same value as at room temperature [7, 20]. Indeed, no intrinsic dependence on temperature is expected on metals, since the excitations producing secondary electrons involve energies of several eV and are not affected by changes in electron band occupancy within a range of $k_B T$. Moreover, the scattering governing the mean free path of secondary electrons, at energies where they can escape the solid, are dominated by electron-electron and electron-plasmon interactions and phonons can be almost neglected.

3. Scrubbing and conditioning:

The decrease of δ_{max} with increasing electron irradiation dose [18,21] on an as received surface is well established from laboratory measurements. This phenomenon is called conditioning or beam scrubbing and for copper it can decrease the δ_{max} down to 1.15 for a dose above 10^{-3} C/mm² [19]. The kinetics of the decrease and the ultimate value of δ_{max} depend on the impinging electron energy [18]. The effectiveness of the conditioning depends on materials. For copper surfaces the essential ingredients of conditioning are the electron stimulated desorption (ESD) and the modification of the carbon species on the surface, from hydrocarbon-like to graphitic-like [18, 22, 23]. For stainless steel, scrubbing has been observed in accelerators [24] and in the lab, however with a marked scattering in the dose necessary to reach the lowest SEY [25]. For aluminium and its alloys, the conditioning has a minimum as a function of dose, with a δ_{max} which remains far above 1 [26]. The influence of the surface contamination, the importance of the carbon from air exposure and the origin of the carbon, which is observed to grow in some cases are still topics under investigation.

From the few measurements of conditioning of copper at cryogenic temperatures in the laboratory there are no indications that the mechanism differs intrinsically from the room temperature case [27]. This is plausible considering that the processes inducing conditioning have thresholds of some tens of eV (for the kinetic energy of the impinging electron), like ESD and molecule cracking. The only possible influence of the temperature might come from the most effective physisorption compared to room temperature. At such low temperature (5-20 K) most of the residual gas species condense on the surface, except helium and hydrogen, the latter forming only sub-monolayer coverages. On one hand adsorbates can strongly modify the SEY [7, 20] of the surface. On the other hand the longer sojourn time of the molecules, compared with room temperature, could increase the amount of adsorbates available for interaction with the impinging electrons and therefore modify the surface chemical composition as a function of

dose. The comparison of laboratory measurements with the real case of a cryogenic accelerator vacuum system is difficult from this point of view. In the laboratory in most of the configurations a small cold sample is acting as a cryopump in a room temperature vessel, whose walls are source of gases, whereas in an accelerator cryogenic vacuum system the entire environment is cold and gases can come only from particle induced desorption. The domain of conditioning at low temperature in presence of gases is still under investigation [28]

ENERGY SPECTRUM OF EMITTED ELECTRONS

In a calculation of the electron multiplication in a beampipe it is necessary to know the detailed energy distribution of the emitted electrons, in order to recalculate their impact energy on the opposite surface. There is no simple theory describing the shape of the spectrum. For the low E_s energy part including the secondary electrons, various parametrizations have been proposed [29, 14, 30]. The simplest one is a decay with a power law of the energy corrected with the work function [29], which was derived from a phenomenological model. To obtain a better matching with data Maxwell-Boltzmann distribution was proposed, which evolved in a Gaussian distribution [14, 11] with energy and finally with the logarithm of energy [30]. This gives the following expression (total integral spectrum normalized to 1):

$$I(E_p, E_s) = \frac{2}{E_s \sigma \sqrt{2\pi}} e^{-\frac{(\ln(E_s - \mu))^2}{2\sigma^2}}$$

Where μ and σ are defining the maximum and the width of the curve, without further physics meaning. We remark that there is no dependence from E_p , which is a reasonable approximation when the secondary electrons are produced with a large number of collisions, as for E_p above some hundredths of eV (confirmed experimentally above 1keV for instance for Si [31]).

The measurement of $I(E_s, E_p)$ can be carried out in principle in any surface analysis system with an electron gun and an energy analyser, but three aspects should be considered. First, the angle of collection depends on the type of energy analyser. In the case of a retarding field analysers (RFA) a large collection angle is available, ideally 180 degrees (in practice some 110 degrees), whereas hemispherical analysers collect a small solid angle. Therefore, in the latter case the total number of emitted secondary electrons must be extracted by assuming a cosine distribution (see next section: Angle dependence) of the secondary electron emission. There is no such simple scaling for elastically scattered electrons. Second, the electron energy analysers have an energy dependent transmission function, which should be calibrated or calculated. Only in this way the spectrum will be weighted with a constant amplification factor or sensitivity. Third, the acquisition of a spectrum or of many spectra for different E_p values, shall be done by limiting the irradiation dose to the surface to avoid conditioning. This last point is not relevant for a sputter cleaned

surface, but is particularly important for an as-received surface.

For copper only few measurements of this spectrum $I(E_s, E_p)$ for normal incidence and a calibrated transmission function exist. A set of data obtained with a RFA for a fully conditioned copper surface at cold are presented in [32]. Other measurements on a larger series of as-received metals were taken, for $E_p=1\text{keV}$ and E_s up to 50eV, with a cylindrical mirror analyser (the intensity is multiplied by the kinetic energy to compensate for transmission) [31] show that the shape of the intensity decrease as a function of E_s strongly depend on the material (see steel vs other metals). Obviously, the spectrum for a specific surface should be measured on purpose.

ANGLE DEPENDENCE

1. Incidence angle dependence of the SEY :

For a flat surface a more grazing incidence angle increases the SEY. An off-normal angle of incidence reduces the depth at which the primary electrons excite the secondary electrons in the solid and therefore the latter can more easily escape than for normal incidence. Compared with the normal emission case, the energy of the maximum, E_{\max} , shifts to higher energy, since the secondary electrons still manage to escape the solid even when excited by higher primary energies. This effect can be strongly reduced on a rough surface, since at microscopic level electrons encounter a wide distribution of angles of incidence. For an as received and air exposed metallic surface the change of depth of the excitation of secondary electrons translates also in a different balance in the number of electrons excited in the metal, in the oxide and in the overlayer of airborne contamination.

In a parametrization of the SEY(E_p) curve like (3) one can introduce an incident angle dependence for $\delta_{\max}(\theta_{inc})$ and $E_{\max}(\theta_{inc})$ to obtain the full curve for any angle. Empirical formulas for such dependences can be found with the introduction of more [11] or less parameters, some including also the possibility to tune for the surface roughness [33]. They are based on available experimental data of SEY measured on different materials, as TiN in the case of [11] and metallic molybdenum [34] in the case of [33]. In another approach the angle dependence is included in an empirical model of SEY(E_p), by considering that the range of the incident beam changes with the cosine of the angle [35]: the scaling of the SEY(E_p) curve is a little more complex in this case. The influence of the different parametrization of the θ_{inc} angle dependence in the electron cloud simulation is partly illustrated in reference [36, 37].

The amount of experimental data of $\delta_{\max}(\theta_{inc})$ is scarce. Some are collected in figure 3, where the maximum yield measured at various incidence angles is normalised by the δ_{\max} at normal incidence (data quoted as belonging to rough surfaces were excluded). This illustrates the possible error when extrapolating from normal incidence data: the angle dependence of reference 33 for a smooth surface

seems to be too weak in most of the cases. The spread increases by increasing the incident angle.

In the electron cloud case the secondary electrons emitted from the wall are accelerated toward the opposite surface of the beampipe by the beam potential. For sufficiently strong dipole magnets the trajectory of the electrons is a cyclotron rotation with the axis parallel to the magnetic field and the speed component parallel to this axis is accelerated. In such a way the impact angles are restricted to a cone close to normal incidence and only the SEY dependence at small angles is important for the e-cloud simulations. This is obviously not true for drift spaces and quadrupoles.

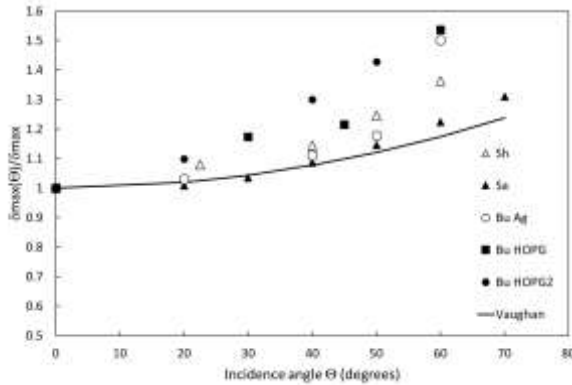


Figure 3: Relative maximum yield as a function of incidence angle. The line corresponds to the model of reference 33, for a smooth surface. The dots are data taken from references 34, 35, 38

In principle a measurement of the SEY(E_p) is possible in most of the set-ups by tilting the sample, but the result should be evaluated with care. In most of the experimental set-ups the sample is biased (either to collect the electrons, or to slow them down, or to avoid recollection of the secondaries) and the electrons do not move in a free field region between gun and sample or between collector and sample.

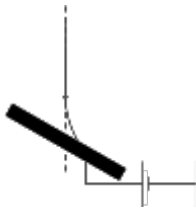


Figure 4: Deviation from straight line for electrons impinging on a sample with a negative bias voltage.

The electric field configuration changes when the sample is rotated with respect to the electron beam. As shown in figure 4 for a sample at negative bias, this situation affects the effective impinging angle of the beam. A suitable correction should be introduced in the measured dependence based on trajectory calculation, which is in practice complicated by the shape of the sample holder. It

is evident that such an effect is more marked for electrons, which are slow compared to the applied bias potential.

2. Incidence and emission angle dependence of the distribution of emitted electrons:

The TEY includes the secondary and elastically scattered electrons, as defined in (2). The secondary electrons are emitted along a distribution, which is very close to a cosine law [10]. This is intuitive if one considers a large amount of collisions, so that the memory of the impinging beam is lost and electrons arrive at the surface from the bulk without preferential direction. The angle dependence of the elastic electrons, $El(E_p, \theta_{inc})$, is not the same as for inelastically scattered. No scaling or simple parametrization exists for this quantity. Elastic scattering as a function of incidence and emission angle at energies above about 100 eV can be calculated from the electron atom scattering cross section [3, 4, 5] in a Monte Carlo calculation, or assuming a single large angle scattering [39] or up to double scattering [40]. A single atomic scattering depends only on the scattering angle between impinging beam and emitted electrons, and is independent of the orientation of the surface. In this sense for angles not too far from normal incidence one can take this approximation [figure 1 d) and e) in 5]. The angular distribution is clearly energy dependent (as visible in all the references just quoted above) and, being related to the atomic structure, it is strongly element dependent. Unfortunately, the extrapolation of the atomic cross sections to energies below 100 eV is no longer meaningful, since the electron wavelength approaches the interatomic distance, atoms cannot be treated as being isolated and band structure and diffraction effects play a role. Measurements of $El(E_p, \theta_{inc})$ are rare and $El(E_p, \theta_{inc}, \theta_{emis})$ are difficult, since they require to change independently the angle between primary beam and electron analyser. A nice solution is adopted in [41] where the relative (arbitrary units) distribution of elastically reflected electrons as a function of primary energy and emission angle is extracted from the fluorescence intensity on a LEED screen. The dataset shows the θ_{emis} angle and E_p dependence for clean polycrystalline Al, Cu, Pt and Au [fig 3 in 41] for normal incidence. The intensity does not exhibit a monotonic behaviour with respect to E_p and the increase below 100eV is not a general feature. Moreover, for normal incidence the scattered intensity is generally stronger at small θ_{emis} angles close to surface normal (backscattering). Also for elastic scattering the presence of adsorbates or oxides on the surface can change the picture completely, since the elastic mean free path is limited to few atomic layers.

MAGNETIC FIELD

The question about the influence of the magnetic field on TEY is motivated by the presence of dipole and quadrupole fields in most of the regions of circular accelerators. Axial magnetic fields (solenoids or permanent magnets) are often exploited to eliminate the electron cloud effect, since they avoid that emitted secondary electrons cross the

vacuum chamber and promote multiplication [42, 43]. For dipole fields we can consider the case of a uniform field perpendicular to the surface. In this case, the electrons cross the vacuum chamber on a helical trajectory with the axis perpendicular to the surface. Only the direction of the speed component parallel to the surface is modified and the speed vectors rotates on a cone (figure 5) for a cyclotron orbit (we neglect here for simplicity the effect of the acceleration by the field of the beam, but the argument does not change). Thus, the angle of incidence with respect to the surface normal is not modified by such a magnetic field. For this reason also the depth of excitation of secondary electrons is not modified: the penetration of the primary electron is just the time between scattering events times the speed component perpendicular to the surface and both quantities are not modified by the magnetic field.

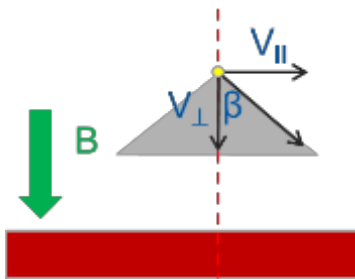


Figure 5 Effect of a magnetic field perpendicular to the surface on the speed of an impinging electron

For quadrupole fields the situation is different, since the field is not uniform in space. As resulting from a calculation in the guiding centre (adiabatic) approximation [44], this can provoke a modification of the relative intensities of the perpendicular and parallel components of the speed. As a consequence the impinging angle changes toward a more grazing direction and in the extreme case the electron can even be reflected by the surface, so that it will remain long time travelling in the field (magnetic bottle). In such case the knowledge of the TEY (E_p , θ_{inc}) is important up to large θ_{inc} . A strong magnetic field, as the 9 T intensity of the LHC dipoles strongly reduces the Larmor radius and one could imagine that it affects the secondary electron cascade. Relevant secondary electrons, which can escape the solid, have a kinetic energy above the work function level. In the solid they have therefore at least a kinetic energy corresponding to the sum of work function and Fermi energy, in total more than 10eV. The corresponding Larmor radius is of the order of microns whereas the mean free path of electrons between two inelastic scattering events is of the order of nanometers [45]. It is clear that the trajectory deviation due to the magnetic field between two scattering events is negligible and therefore there is no intrinsic dependence of the SEY for a flat metal in the mentioned range of field. Measurements of TEY in a magnetic field are very difficult due to deviation induced on the secondary electrons escaping in vacuum. There are only few measurements at low magnetic field [17, 46]. The results up to fields of few tens of mT [46] on a smooth sample confirm

that there is no intrinsic dependence, however even the minor roughness on a laminated sample is sufficient to induce a decrease of TEY as a function of the field strength.

CONCLUSIONS

As illustrated above the dependence of the intensity and distribution of the emitted electrons on the energy and direction of the impinging electrons is influenced by surface and material properties. Only few aspects can be generalised and expressed with sufficient reliability through a parametrization. In most of the cases, a measurement is the most reliable approach even if it is not always easy and straightforward. In particular, measurements should be done by taking into account the dose received by the surface, the transmission function of the analysers in case of angle and energy resolved experiments and the influence of the geometry of the measuring system.

ACKNOWLEDGMENTS

It is a pleasure for the author to acknowledge fruitful discussions with V.Petit, G.Iadarola, H.Neupert, D.Zanin and M.Himmerlich as well as with many participants of the ECLLOUD 18 workshop.

REFERENCES

- [1] ESA multipactor tool from ESA/ESTEC, <http://multipactor.esa.int/>
- [2] G. Iadarola, E. Belli, K. Li, L. Mether, A. Romano, G. Rumolo, Evolution of PYTHON tools for the simulation of electron cloud effects, proceedings IPAC 2017, p. 3803, Copenhagen Denmark
- [3] J. Pierron, PhD thesis Université de Toulouse France, Modèle de transport d'électrons à basse énergie pour applications spatiales, 2017
- [4] M. Azzolini, M. Angelucci, R. Cimino, R. Larciprete, N. M. Pugno, S. Taioli, M. Dapor: "Secondary electron emission and yield spectra of metals from Monte Carlo simulations and experiments", J.Phys. Cond. Mat. 31 (5) Art. No. 055901 (2019)
- [5] E.Kieft, E.Bosch, Refinement of Monte Carlo simulations of electron-specimen interaction in low-voltage SEM, J.Phys. D, Appl.Phys 41 (2008) 215310
- [6] I. Bojko, N.Hilleret, C. Scheuerlein, Influence of air exposures and thermal treatments on the secondary electron yield of copper, J.Vac. Sci.Technol. A18, 972 (2000)
- [7] A. Kuzucan, H.Neupert, M.Taborelli, H. Störi, Secondary electron yield on cryogenic surfaces as a function of physisorbed gases, J.Vac. Sci.Technol. A30, 051401 (2012)
- [8] S. Calatroni, E. Garcia-Tabares Valdivieso, H.r Neupert, V. Nistor, A. T. Perez Fontenla, M. Taborelli, P. Chiggiato, O. Malyshev, R. Valizadeh, S. Wackerow, S. A. Zolotovskaya, W. A. Gillespie, A. Abdolvand, First accelerator test of vacuum components with laser-engineered surfaces for electron-cloud mitigation, PRST AB 20, (2017) 113201
- [9] A.J. Dekker, Solid State Physics, ed. F. Seitz, D. Turnbull, H. Ehrenreich, Academic Press, NY, VI, 251 (1958).

- [10] H.Seiler, Secondary emission in the scanning electron microscope, *J.Appl.Phys*, 54 R1 (1983)
- [11] M.Furman, M.T.F. Pivi, Probabilistic model for the simulation of secondary electron emission PRST AB, 5, 124404 (2002)
- [12] Yee-Rendon*, R. Muto, K. Ohmi, M. Okada, K. Satou, M. Tomizawa and T. Toyama, PYecloud simulations of the electron cloud for the J-Parc main ring, Proc. 14th Annual Meeting of Particle Accel. Soc. Japan, Sapporo (2017) p. 197 https://www.pasj.jp/web_publication/pasj2017/proceedings/PDF/THOM/THOM07.pdf
- [13] R. Cimino, I.R.Collins, M.A.Furman, M.Pivi, F.Ruggiero, G.Rumolo and F.Zimmermann, Can low-energy electrons affect high-energy physics accelerators, *Phys.Rev.Lett*, 93, 014801, (2004)
- [14] Scholtz, J.J., D. Dijkkamp, and R.W.A. Schmitz, *Philips Journal of Research*, 1996. 50(3-4), 375
- [15] V.Baglin, I. Collins, B.Henrist, N.Hilleret and G.Vorlauer, A summary of main experimental results concerning the secondary electron emission of copper, LHC project report 472, CERN, Geneva (2002)
- [16] R. Cimino, A. Di Gaspare, L. Gonzalez, and R. Larciprete, Detailed investigation of the low-energy secondary electron yield, *IEEE Trans. Plasma Sci.*, 43, 2015, 2954
- [17] V. V. Anashin, A. A. Krasnov, V.K. Ovchar, V.V.Smaluk, D.P.Sukharov, Installation for measurement of secondary emission yield and electron cloud lifetime in magnetic field, DIPAC 2011, Hamburg
- [18] R.Cimino, M.Commisso, D.R.Grosso, T.Demma, V.Baglin, R.Flammini and R. Larciprete, Nature of the decrease of the secondary electron yield by electron bombardment and its energy dependence, *Phys.Rev.Lett*, 109, 064801 (2012)
- [19] V.Petit, ECLLOUD 18 workshop, 3-7 June 2018, La Biodola, Elba Island, Italy
- [20] L. A. Gonzalez, M. Angelucci, R. Larciprete and R. Cimino, "The secondary electron yield of noble metal surfaces," *AIP Advances*, vol. 7, p. 115203, 2017
- [21] V.Baglin, I. Collins, B.Henrist, N.Hilleret and G.Vorlauer, A summary of main experimental results concerning the secondary electron emission of copper, LHC project report 472, CERN, Geneva (2002)
- [22] C. Scheuerlein and M. Taborelli, "Electron stimulated adsorption in ultrahigh vacuum monitored by Auger electron spectroscopy," *Journal of vacuum science & technology A*, vol. 20, no. 1, pp. 93-101, 2002
- [23] M. Nishiwaki and S. Kato, "Graphitization of inner surface of copper beam duct of KEKB positron ring," *Vacuum*, vol. 84, pp. 743-746, 2010
- [24] Yin Vallgren, G. Arduini, J. Bauche, S. Calatroni, P. Chiggiato, K. Cornelis, P. Costa Pinto, B. Henrist, E. Métral, H. Neupert, G. Rumolo, E. Shaposhnikova, and M. Taborelli, Amorphous carbon coatings for the mitigation of electron cloud in the CERN Super Proton Synchrotron, *Phys Rev. ST Accel Beams* **14**, 071001 (2011)
- [25] R.Cimino, ECLLOUD 18 workshop, 3-7 June 2018, La Biodola, Elba Island, Italy
- [26] F.Le Pimpec F.King, R.E.Kirby and M.Pivi, Electron conditioning of technical aluminium surfaces: effect on secondary electron yield, *J. Vac. Sci. Technol. A* **23**, 1610 (2005)
- [27] V. Baglin, The LHC vacuum system: Commissioning up to nominal luminosity, *Vacuum* 138 (2017) 112
- [28] B.Henrist, ECLLOUD 18 workshop, 3-7 June 2018, La Biodola, Elba Island, Italy
- [29] M.S.Chung, T.E.Everhart, Simple calculation of energy distribution of low energy secondary emission from metals, *J.Appl.Phys* 45 (1974), 707
- [30] G.Rumolo, F.Zimmermann, E-cloud simulations: build up and related effects, Proceedings of ECLLOUD02, CERN, Geneva (2002), p 97
- [31] D.C.Joy, M.S.Prasad, H.M.Meyer, Experimental secondary electron spectra under SEM conditions, *Journal of Microscopy*, 215 (2004) 77
- [32] R. Cimino, I.R.Collins, Vacuum chamber surface electronic properties, *Appl. Surf. Sci.* 235 (2004) 231–235
- [33] J.R.M. Vaughan, *IEEE Trans El Dev* 40, 830, (1993) and 36, 1963, (1989)
- [34] A.Shih and C.Hor, Secondary emission properties as a function of the electron emission angle *IEEE Trans. El. Electron Dev*, 40, (1993) 824
- [35] N.Bundaleski, M.Belhaj, T.Gineste, O.Teodoro, Calculation of the angular dependence of the total electron yield, 122 (2015) 255
- [36] D. Astapovych, ECLLOUD 18 workshop, 3-7 June 2018, La Biodola, Elba Island, Italy
- [37] L.Sabato, ECLLOUD 18 workshop, 3-7 June 2018, La Biodola, Elba Island, Italy
- [38] M.Salehi, E.A.Flinn, Dependence of secondary electron emission from amorphous materials on primary angle of incidence, *J.Appl. Phys.* 52 (1981) 994
- [39] A.Jablonski, Analytical theory of elastic electron backscattering from elements alloys and compounds: comparison with experimental data, *J. Electr. Spectr. Rel.Phenom.* 206 (2016), 24
- [40] W.Werner, I.Tilinin, M.Hayek, Angular distribution of electrons reflected elastically from nanocrystalline solid surfaces *Phys. Rev.B*, 50 (1994) 4819
- [41] A.Jablonski, P.Jiricek Elastic Electron Backscattering from surfaces at low energies, *Surf. Interf.Analysis* 24, (1996) 781
- [42] Y. Suetsugu, K. Shibata, T. Ishibashi, K. Kanazawa, M. Shirai, S. Terui, and H. Hisamatsu, First commissioning of Super KEKB vacuum system, PRST AB, 19, 121001 (2016)
- [43] R.J. Macek, Possible cures for electron cloud problems, proceedings of ECLLOUD02, CERN, Geneva (2002), p 259
- [44] M. Moisan, J. Pelletier, Individual Motion of a Charged Particle in Electric and Magnetic Fields. *Physics of Collisional Plasmas*. Springer (2012) Dordrecht
- [45] M.P.Seah, W.A.Dench, Quantitative electron spectroscopy of surfaces: a standards database for electron inelastic mean free paths in solids, *Surf. Interf. Anal.* 1, (1979), 2
- [46] N.Fil, PhD thesis Université de Toulouse France, Caractérisation et modélisation des propriétés d'émission électronique sous champ magnétique pour des systèmes RF hautes puissances sujets à l'effet multipactor, 2017